1990

Optimum Operating Pressure Ratio for Scroll Compressor

T. Yanagisawa
Shizuoka University

M. D. Cheng
Shizuoka University

M. Fukuta
Shizuoka University

T. Shimizu
Shizuoka University

OPTIMUM OPERATING PRESSURE RATIO FOR SCROLL COMPRESSOR

Tadashi YANAGISAWA, Associate professor
CHENG Min Chi, Visiting lecturer from China
Mitsuhiro FUKUTA, Research Associate
Takashi SHIMIZU, Professor

Department of Energy and Mechanical Engineering,
Shizuoka University,
3-5-1, Johoku, Hamamatsu, Shizuoka, 432, JAPAN

ABSTRACT

A scroll compressor has a built-in pressure ratio related to geometry of scroll wraps and efficiency of the compressor depends on the relation between the ratio and an operating pressure ratio. This paper analyses theoretical performance of the compressor by taking account of flow resistances at openings of scroll wraps and leakage flows through wrap clearances. The flow resistance at the discharge opening causes an overcompression loss at a built-in pressure ratio operation but it reduces an undercompression loss at a high pressure ratio operation, which leads an optimum operating pressure ratio higher than the built-in pressure ratio. Leakages accelerate pressure rise during a compression process and reduces the compressor efficiency more at a higher pressure ratio operation.

NOMENCLATURE

A_s, A_d: flow areas of suction and discharge openings
A_p : flow area of discharge port
a : basic circle radius
b : thickness of wrap
c : flow coefficient
d : discharge port diameter
h : height of wrap
L : average compression power
ℓ_a, ℓ_b: lengths of tangent lines from points on inner and outer curves
ℓ_l : sealing line length of tip leakage
m : mass of gas in pocket
$\dot{m}$: mass flow rate
$\dot{m}_s$: effective suction mass flow rate
N : rotational speed of shaft
P : pressure of gas in pocket
P_s, P_d: suction and discharge pressure
r : radius of revolution
r_a : radius of starting circular arc
T : torque of crank shaft
T_{ad}: adiabatic compression torque
t : time
V : volume of pocket
V_0 : volume of discharge pocket (V_{00}, V_{01}:divided discharge pocket volumes)
V_c : clearance volume
V_n, V_1: volumes of suction and compression pockets
V_s, V_d: theoretical suction and discharge volumes
w_s, w_d: widths of suction and discharge opening
α : involute angle corresponding to half of wrap thickness
δ_a : tip clearance between wrap tip and base plate
δ_r : flank clearance between wrap walls
ε_p : built-in pressure ratio
η_{ad}: adiabatic compression efficiency
θ : rotational angle
θ_d : rotational angle at discharge starting
κ : adiabatic compression exponent
ρ_s : density of suction gas
ϕ : involute angle
ϕ_s, ϕ_e: involute starting and ending angles
ω : angular velocity of rotation

INTRODUCTION

Scroll machinery[1] which is a kind of positive displacement type fluid machinery has been put into practical use as a compressor and many researches and developments[2]-[15] on them are carried out for improvements of the performance and new applications.

A scroll compressor, which has constant suction and discharge volumes decided by geometry of scroll wraps, is a so-called compressor having a constant built-in volume ratio. The compressor can operate without any valves but in that case efficiency of the compression changes depending on the relation between an operating pressure ratio and a built-in pressure ratio that is a function of the built-in volume ratio. Ideally it is desirable to operate the compressor under the built-in pressure ratio but practically it is not always preferable because of internal pressure loss and leakage loss.

This paper analyses theoretical pressure changes in wrap pockets based on the geometry and investigates performance of the compressor by considering flow resistances at openings of scroll wraps and leakage flows through wrap clearances. An optimum operating pressure ratio which maximizes efficiency of the compressor is examined by changing wrap clearances and the rotational speed.

THEORETICAL ANALYSIS

Ideal Performance

Figure 1 shows a schematic view of a scroll wrap which is formed by involute curves. The length of a tangent line from a point on an inner or outer involute curve to a basic circle at involute angle ϕ is expressed as follows.

$$\ell_a = a(\phi - \alpha) \tag{1}$$

$$\ell_b = a(\phi + \alpha) \tag{2}$$

Where $\alpha=b/(2a)$. The inner involute curve develops from involute angle Φ_a to Φ_e and the outer curve from $(\Phi_a-\pi)$ to ϕ_e. At a central part of the wrap the inner curve continues smoothly to a circular arc with radius, r_a $[=a\{\phi_a - \pi/2 + 1/(\phi_a - \pi/2)\}]$.

Figure 2 shows a combination of a fixed scroll wrap and an orbiting scroll wrap which revolves with radius, r (=πa-b), around a center of the fixed scroll. A compression process starts at rotational angle $\theta=0$ every revolution and it ends at $\theta=\theta_d$ defined by the next equation.

$$\theta_d = \Phi_e - \Phi_a - 2\pi INT\{(\Phi_e - \Phi_a)/(2\pi)\} \tag{3}$$

At a rotational angle, θ, there exist n $[=INT\{(\Phi_e - \theta - \Phi_a)/(2\pi)\} + 1]$ pairs of contact points and (n-1) pairs of compression pockets. Involute angle, Φ_i, of i-th contact point from center on the inner curve is given as follows.

$$\Phi_i = \Phi_e - \theta - 2\pi(n - i) \tag{4}$$

Volume, V_n, of a pair of suction pockets, volume, V_i, of a pair of compression pockets formed between i-th and (i+1)-th contact points, and volume, V_0, of a discharge pocket are expressed as follows by geometrical relation.

$$V_n = 2h\{\frac{1}{2}\int_{\Phi_n}^{\Phi_e} \ell_a^2 d\phi - \frac{1}{2}\int_{\Phi_n-\pi}^{\Phi_e-\pi} \ell_b^2 d\phi + \text{area}(2345)\}$$

$$= 2ar\{\theta(2\Phi_e - \theta - \pi) - 2(\Phi_e - \pi + \alpha)\sin\theta - (\pi/2 - \alpha)\sin(2\theta) + 2(1 - \cos\theta)\} \tag{5}$$

$$V_i = 2h(\frac{1}{2}\int_{\Phi_i}^{\Phi_i+2\pi} \ell_a^2 d\phi - \frac{1}{2}\int_{\Phi_i-\pi}^{\Phi_e+\pi} \ell_b^2 d\phi) = 2\pi ar(2\Phi_i + \pi) \tag{6}$$

$$V_0 = 2h(\frac{1}{2}\int_{\Phi_a}^{\Phi_1} \ell_a^2 d\phi - \frac{1}{2}\int_{\Phi_a-\pi}^{\Phi_1-\pi} \ell_b^2 d\phi) + V_c = ar(\Phi_1 - \Phi_a)(\Phi_1 + \Phi_a - \pi) + V_c \tag{7}$$

Where, V_c [$=hr_a^2\{\pi - \sin^{-1}(2a/r_a) - (2a/r_a)\}$] is a clearance volume {$=V_0(\Phi_1=\Phi_a)$}. Theoretical suction and discharge volumes, V_s and V_d, of the compressor are given by putting $\Phi_i=\Phi_e-2\pi$ and $\Phi_i=\Phi_a$ in equation (6) respectively.

When the scroll compressor operates ideally, pressure, P_n, in the suction pocket and pressure, P_0, in the discharge pocket are equal to suction pressure, P_s, and discharge pressure, P_d, of the compressor respectively, and pressure, P_i, in the compression pocket is given by the next equation.

$$P_i = P_s(V_s/V_i)^K \tag{8}$$

An instantaneous torque, T, of a crank shaft to drive the orbiting scroll and an average power, L, of the shaft are derived as follows.

$$T = -\sum_{j=0}^{n}(P_j - P_s)dV_j/d\theta = har\{(2\Phi_1-\pi)(P_d-P_s) + 4\pi\sum_{J=1}^{n-1}(P_j-P_s)\} \tag{9}$$

$$L = \frac{\omega}{2\pi}\int_0^{2\pi} Td\theta \tag{10}$$

Practical Performance

In a practical compressor, pressures in scroll pockets differ from ideal pressures because of pressure losses in flowing into and out of pockets and internal leakages through wrap clearances. At that time pressure, P_j, in a pocket with volume, V_j, is evaluated as an adiabatic compression.

$$P_j = (P_s/\rho_s^K)(m_j/V_j)^K \tag{11}$$

Where ρ_s is density of suction gas, and mass, m_j, of gas in the pocket is expressed by summation of integrated mass flow rates which flow into or out of the pocket in many ways mentioned below.

$$m_j = \sum\int_0^t \dot{m}dt \tag{12}$$

Each mass flow rate is examined as follows. At first, a mass flow rate through suction openings formed by terminals of the wraps is rated by the next equation.

$$\dot{m} = 2chw_s f(P_s,P_n) \tag{13}$$

where c is a flow coefficient and $f(P_1,P_2)$ is a mass flow rate of isentropic flow through an orifice with unit area from one chamber with pressure, P_1, to another chamber with pressure, P_2. A width of the suction opening is expressed as follows based on geometry in Figure 2.

$$w_s = \overline{12} = \overline{13} - \overline{23} = r(1-\cos\theta) \tag{14}$$

Concerning a discharge process, a mass flow rate through a discharge port located on a base plate of the fixed wrap is expressed as follows.

$$\dot{m} = c(\pi/4)d^2 f(P_0,P_d) \tag{15}$$

But at earlier part of the discharge process, the discharge flow is limited by discharge openings formed by starting points of the wraps as shown in Figure 3. Then, a discharge mass flow rate, $\dot{m}$, a width, w_d, of the discharge opening, volumes, V_{00} and V_{01}, of conveniently divided discharge pockets are expressed as follows.

$$\dot{m} = 2chw_d f(P_{01},P_{00}) \tag{16}$$

$$w_d = \overline{12} = \overline{13} - \overline{23} = r_a - \sqrt{r^2 + (r_a-r)^2 + 2r(r_a-r)\cos(\theta-\theta_d)} \tag{17}$$

$$V_{00} = 2h\{\text{area}(132') - \text{area}(232')\} = hr_a\{r_a\beta - (r_a-w_d)\sin\beta\} \tag{18}$$

where $\beta = \pi - \cos^{-1}[\{r_a - r + r\cos(\theta-\theta_d)\}/(r_a-w_d)] - \sin^{-1}(2a/r_a)$

$$V_{01} = V_0 - V_{00} \tag{19}$$

On the other hand, concerning leakages through wrap clearances, there exist two kinds of leakage flow, one is through tip clearance, δ_a, between a wrap tip and a base plate and the other is through flank clearance, δ_r, between wrap walls. The leakage mass flow rate is expressed as follows.

$$\dot{m} = 2c(h\delta_r + \ell_j\delta_a)f(P_{j-1},P_j) - 2c(h\delta_r + \ell_{j+1}\delta_a)f(P_j,P_{j+1}) \tag{20}$$

Where ℓ_j is a sealing line length of the tip leakage between j-th and (j+1)-th pockets.

$$\ell_j = \int_{\phi_j-\pi}^{\phi_j} a\phi d\phi = \pi a(\phi_j - \pi/2) \tag{21}$$

By taking account of these mass flow rates, pressures in wrap pockets are calculated from equation (11), which enables to estimate an instantaneous torque by equation (9) and an average power by equation (10). Also an effective suction mass flow rate, $\dot{m}_s$, is given by subtraction of leakage mass flow rate from mass flow rate through suction opening. Then, a theoretical adiabatic compression power, L_{ad}, and an adiabatic efficiency, η_{ad}, of the compressor are given as follows.

$$L_{ad} = \{\kappa/(\kappa-1)\}P_s(\dot{m}_s/\rho_s)\{(P_d/P_s)^{1-1/\kappa} - 1\} \tag{22}$$

$$\eta_{ad} = L_{ad} / L \tag{23}$$

Calculations above mentioned are executed by iteration for each small increment of rotational angle.

RESULTS AND DISCUSSIONS

Dimensions of a scroll wrap used for theoretical calculations are; basic circle radius:a=3 mm, wrap thickness:b=4.6 mm, wrap height:h=29.4 mm, involute starting angle:ϕ_a=1.09π rad, involute ending angle:ϕ_e=5.59π rad, radius of starting circular arc:r_a=7.2 mm, clearance volume:V_c=2.0 cm^3, discharge port diameter:d=10 mm, theoretical suction volume:V_s=68.7 cm^3, theoretical discharge volume:V_d=26.7 cm^3. Conditions of calculation supposing that the compressor is operated in an air conditioning cycle using HCFC 22 as a working fluid are; compression exponent:κ=1.1, suction pressure:P_s=584 kPa[abs] (corresponding to saturation temperature 5°C), suction gas density:ρ_s=23.5 kg/m^3 (corresponding to 15°C), discharge pressure:P_d=(2 ~ 5) ×P_s, standard rotational speed:N=3500 rpm. In the following calculation, every flow coefficient, c, is assumed to be equal to 1.

Influence of Flow Resistance on Performance

Figure 4 shows relationships between pressure, P_j, in wrap pocket and shaft torque, T, and rotational angle, θ, under an operating pressure ratio, P_d/P_s, equal to a built-in pressure ratio, $\varepsilon_o(=(V_s/V_d)^\kappa=2.83)$. In the figure the pressure and the torque are normalized by a suction pressure, P_s, and an average adiabatic compression torque, $T_{ad}[=\{\kappa/(\kappa-1)\}P_sV_s\{(P_d/P_s)^{1-1/\kappa} - 1\}/(2\pi)]$, respectively. As shown in Figure 4, the flow resistance at discharge opening causes a large overcompression during a discharge process even if that of a discharge port causes little overcompression. This is because, as shown in Figure 5, a discharge opening area, A_d (=2hw_d), is very little immediately after the discharge starting ($\theta=\theta_d$) while a discharge port area, A_p (=πd^2/4), is constant. Then a discharge pocket is divided by the discharge opening into two rooms, V_{00} and V_{01}, and a pressure in the room, V_{01}, rises greatly but a pressure in the other room, V_{00}, shows little overcompression as shown in Figure 4. This overcompression increases a torque during the discharge process.

In Figure 4 the flow resistance at suction opening elevates a pressure at suction process ending ($\theta=2\pi$), which leads to pressure rise during a compression process. This is because, as shown in Figure 5, a volume, V_n, of suction pocket begins to decrease before a suction process ending while a suction opening area, A_s (=2hw_s), becoming very small prevents a back flow. This increases volumetric efficiency and shifts the torque curve upward as shown in Figure 4. When both flow resistances at suction and discharge openings are taken into consideration, their effects are superimposed and more overcompression is caused.

Figure 6 shows influence of operating pressure ratio, P_d/P_s, on the pressure

and torque curves by taking account of suction and discharge flow resistances. Under the ideal condition a discharge pressure changes in a stepwise manner at discharge process starting. But when the flow resistances are considered, an overcompression becomes very large at an operating pressure ratio(=2.5) lower than a built-in pressure ratio, ε_p(=2.83), which increases amplitude of torque fluctuation. On the other hand, at higher pressure ratio operation, the discharge pressure rises smoothly as an extension of the compression process and the overcompression becomes small as the pressure ratio increases.

Figure 7 shows relationships between operating pressure ratio, P_d/P_s, and adiabatic compression efficiency, η_{ad}, calculated by taking account of suction and discharge flow resistances. At an ideal condition the efficiency shows maximum value of 100 % at a built-in pressure ratio, ε_p. When the suction resistance is considered, the efficiency curve lowers somewhat and shifts slightly to the right due to the pressure increase during compression process. When the discharge resistance is accounted, the efficiency curve shows its maximum at a rather higher pressure ratio than the built-in pressure ratio. This is because of a large overcompression loss at low pressure ratio and a small undercompression loss at at high pressure ratio. When the both flow resistances are considered, an optimum operating pressure ratio which makes the efficiency maximum becomes still higher and reaches 3.6 in this case. Moreover, the flow resistance makes the efficiency curve flatter though it decreases the maximum efficiency.

Influence of Leakage on Performance

Figure 8 shows influence of leakages through tip and flank clearances of wraps on the pressure and torque curves which include flow resistances. As compared with a case of no leakage ($\delta_a = \delta_r = 0$), the leakage through tip clearance, δ_a, increases a pressure during a compression process but lessens somewhat an overcompression during a discharge process. On the other hand, the leakage through flank clearance, δ_r, accelerates the pressure rise during a later part of the compression process and increases the succeeding overcompression. When the both leakages are considered, the compression process pressure increases more but the overcompression is less than that without leakages. These leakages increase an average of torque as compared with that in Figure 4.

Figure 9 shows the pressure and torque curves at different operating pressure ratios which are calculated by taking account of leakages and flow resistances. As compared with Figure 6 which doesn't include the influence of leakages, the overcompression at low pressure ratio (=2.5) operation is moderated but the pressure rise during a compression process becomes early as the pressure ratio increases. Then the corresponding torque increases on the average though its fluctuation becomes less as compared with Figure 6.

Figure 10 shows relationships between operating pressure ratio and adiabatic compression efficiency which include influences of leakages and flow resistances. As clearances increase, the efficiency curve goes down and shifts to the left. In other words, an optimum operating pressure ratio moves to low pressure ratio with increasing leakage. The reason is that the leakage loss at a constant clearance becomes large as the operating pressure ratio increases.

Influence of Rotational Speed on Performance

Figure 11 shows influence of rotational speed, N, on the pressure and torque curves including flow resistances but excluding leakages. As the rotational speed increases, an overcompression becomes large due to a larger flow rate, which increases a fluctuation of torque curve. On the other hand, a pressure during a suction process becomes slightly low but a pressure during a compression process is almost the same. Then the volumetric efficiency which is decided by a pressure at suction ending increases slightly with increasing rotational speed (volumetric efficiency = 102.8, 103.3, 103.7 % at N=1750, 3500, 7000 rpm) though it decreases definitely at an extremely high speed operation.

Figure 12 shows relationships between operating pressure ratio and adiabatic compression efficiency under different rotational speeds and different clearances. At each constant clearance, the optimum operating pressure ratio shifts to high pressure ratio with increasing the rotational speed though the curve goes upward or downward depending on the existence of leakage. This is because a back flow loss

which occurs through the discharge opening under high pressure ratio operation is depressed due to a larger flow resistance at higher speed operation. By the way, the efficiency curve becomes flatter at higher speed operation, which means that the efficiency becomes less sensitive to the operating pressure ratio around the optimum ratio.

In this paper, flow coefficients are assumed to be equal to 1 for simplicity but the assumption doesn't change qualitative influences of flow resistances and leakages on the performance. Also geometry of the central part of wrap doesn't affect qualitative results as far as the part is not changed greatly such as having a step. However, a consideration of relative position of a discharge port and wraps is needed to more detailed analyses.

CONCLUSIONS

Based on geometry of scroll wraps, influences of flow resistances at suction and discharge openings and leakage flows through tip and flank clearances on the pressure and torque curves were analyzed theoretically. Also an optimum operating pressure ratio which maximizes the compression efficiency was investigated by changing clearances and rotational speed. The results are summarized as follows.

(1) The flow resistance at suction openings elevates a pressure at suction process ending and gives an optimum operating pressure ratio slightly higher than a built-in pressure ratio.

(2) The flow resistance at discharge openings causes an overcompression loss at a built-in pressure ratio operation but reduces an undercompression loss at a high pressure ratio operation, which leads to an optimum operating pressure ratio rather higher than a built-in pressure ratio.

(3) The leakage through tip clearance increases an overcompression loss but the leakage through flank clearance decreases that loss. Both leakages accelerate a pressure rise during a compression process so that an optimum pressure ratio becomes lower than that it would be in absence of leakages.

(4) Increasing of rotational speed increases an overcompression loss at low pressure ratio operation but moderates an undercompression loss at high pressure ratio operation, which leads to a higher optimum operating pressure ratio.

Therefore, dimensions of scroll wrap must be selected such as it has a maximum efficiency at an actual operating pressure condition by taking account of rotational speed and leakage.

REFERENCES

(1) Creux, L., "Rotary Engine", US Pat., No.801182, 1905.
(2) Hiraga, M., "The Special Compressor - An Innovative Air Conditioning Compressor for the New Generation Automobiles", 1983 SAE paper, No.830540.
(3) Morishita, E., et al., "Scroll Compressor Analytical Model", Proc. 1984 Int. Comp. Eng. Conf., 1984, 487.
(4) Tojo, K., et al., "A Scroll Compressor for Air Conditioners", Proc. 1984 Int. Comp. Eng. Conf., 1984, 496.
(5) Bush, J. W., et al., "Dimensional Optimization of Scroll Compressors", Proc. 1986 Int. Comp. Eng. Conf., 1986, 840.
(6) Hayano, M., "Performance Analysis of Scroll Compressor for Air Conditioners", Proc. 1986 Int. Comp. Eng. Conf., 1986, 856.
(7) Ishii, N., "A Study on Dynamic Behavior of a Scroll Compressor", Proc. 1986 Int. Comp. Eng. Conf., 1986, 901.
(8) Caillat, J., et al., "A Computer Model for Scroll Compressors", Proc. 1988 Int. Comp. Eng. Conf., 1988, 47.
(9) Hirano, T., et al., "Development of High Efficiency Scroll Compressors for Air Conditioners", Proc. 1988 Int. Comp. Eng. Conf., 1988, 65.
(10) Bush, J. W., Elson, J. P., "Scroll Compressor Design Criteria for Residential Air Conditioning and Heat Pump Applications", Proc. 1988 Int. Comp. Eng. Conf., 1988, 83.
(11) Nieter, J. J., "Dynamics of Scroll Suction Process", Proc. 1988 Int. Comp. Eng.

Conf., 1988, 165.
(12) DeBlois, R. L., Stoeffler, R. C., "Instrumentation and Analysis Techniques for Scroll Compressors", Proc. 1988 Int. Comp. Eng. Conf., 1988, 182.
(13) Morishita, E., et al., "Rotary Scroll Vacuum Pump", Proc. 1988 Int. Comp. Eng. Conf., 1988, 198.
(14) Yanagisawa, T., et al., "Study on Fundamental Performance of Scroll Expander", Trans. Jpn. Soc. Mech. Eng., B54-506, 1988, 2798.
(15) Etemad, S., Nieter J., "Design Optimization of the Scroll Compressor", Int. J. Refrig., 12-3, 1989, 146.

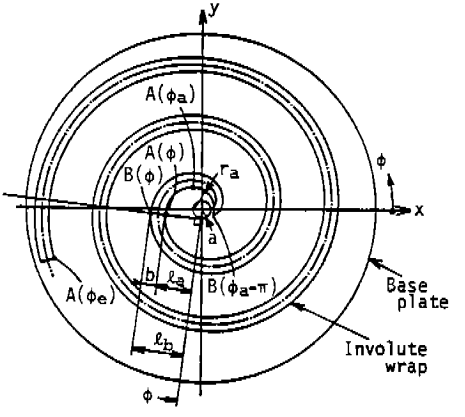

Fig. 1 Outline of involute scroll wrap

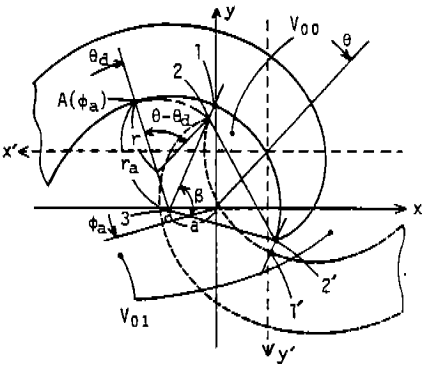

Fig. 2 Combination of fixed and orbiting scroll wraps

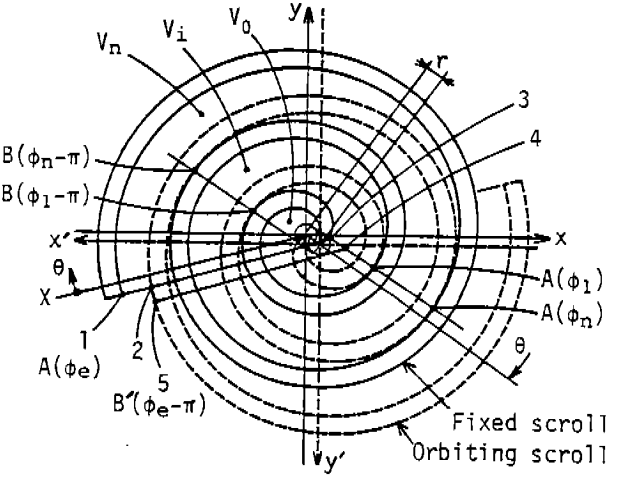

Fig. 3 Details of wrap central parts

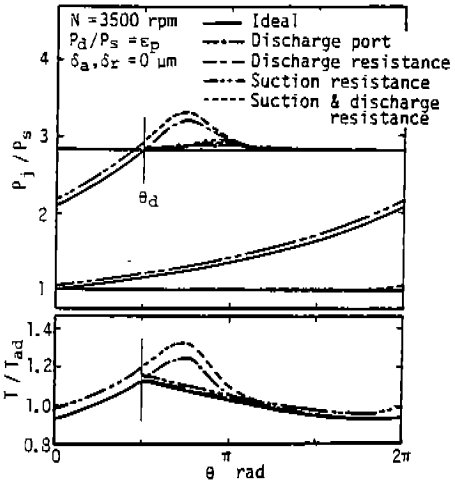

Fig. 4 Influences of flow resistances on pressure and torque at built-in pressure ratio operation

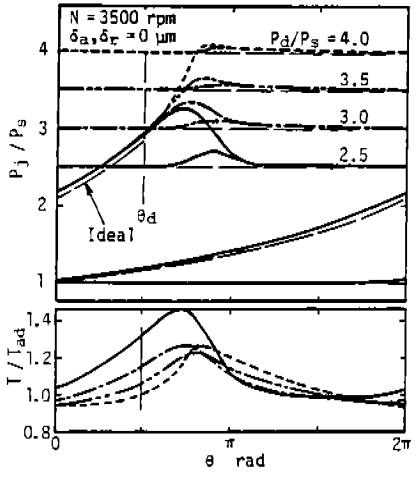

Fig. 6 Influences of flow resistances on pressure and torque at different operating pressure ratios

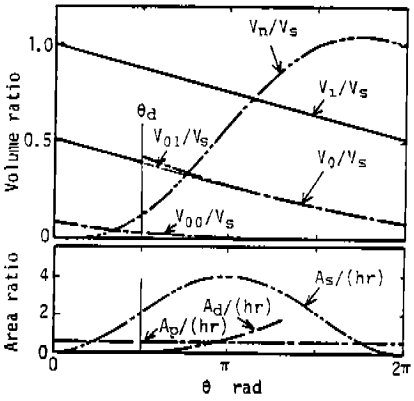

Fig. 5 Diagrams of volume and flow area

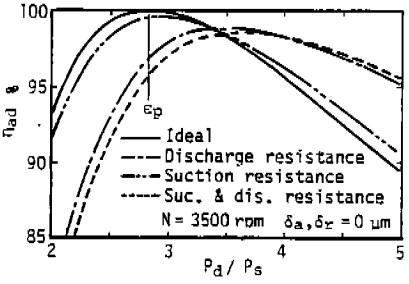

Fig. 7 Relationships between operating pressure ratio and adiabatic efficiency under different flow resistances

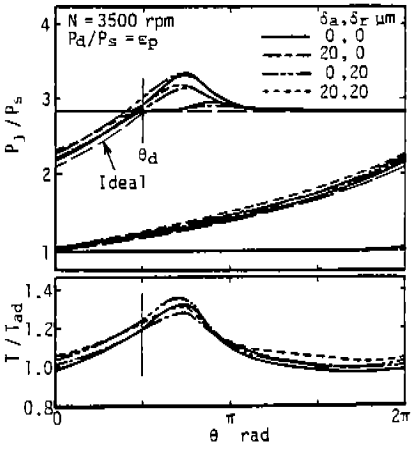

Fig. 8 Influences of leakages on pressure and torque at built-in pressure ratio operation

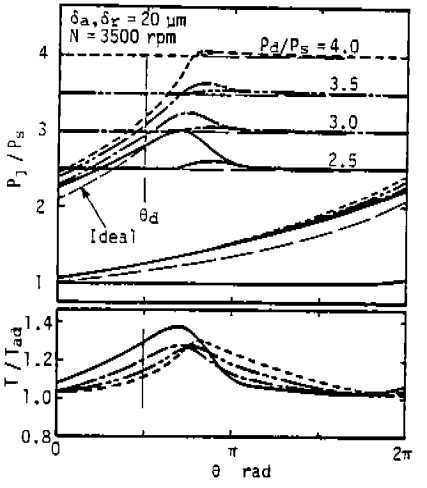

Fig. 9 Influences of leakages on pressure and torque at different operating pressure ratios

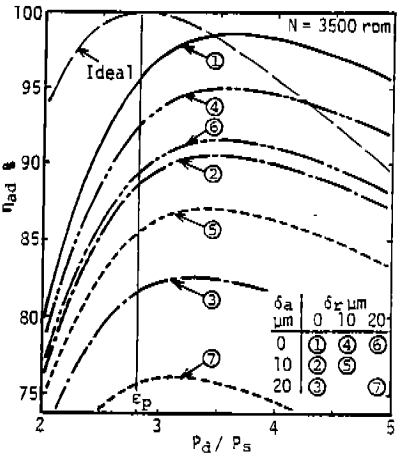

Fig. 10 Relationships between operating pressure ratio and adiabatic efficiency under different clearances

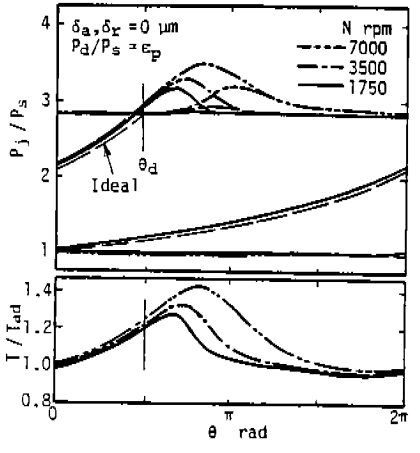

Fig. 11 Influence of rotational speed on pressure and torque at built-in pressure ratio operation

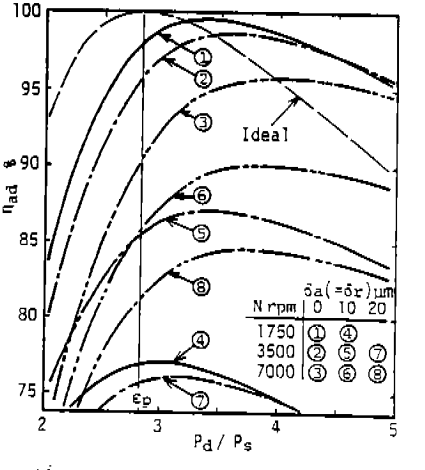

Fig. 12 Relationships between operating pressure ratio and adiabatic efficiency under different rotational speeds and different clearances